

Non-Detection of HC₁₁N toward TMC-1: Constraining the Chemistry of Large Carbon-Chain Molecules

Ryan A. Loomis,^{1*} Christopher N. Shingledecker,² Glen Langston,³
Brett A. McGuire,^{4,5,8} Niklaus M. Dollhopf,^{6,9} Andrew M. Burkhardt,⁶ Joanna Corby,⁶
Shawn T. Booth,^{6,10} P. Brandon Carroll,⁷ Barry Turner,^{4,†} and Anthony J. Remijan⁴

¹*Department of Astronomy, Harvard University, Cambridge, MA 02138*

²*Department of Chemistry, University of Virginia, Charlottesville, VA 22904*

³*National Science Foundation, Division of Astronomical Sciences, Arlington, VA 22230*

⁴*National Radio Astronomy Observatory, Charlottesville, VA 22904*

⁵*Harvard-Smithsonian Center for Astrophysics, Cambridge, MA 02138*

⁶*Department of Astronomy, University of Virginia, Charlottesville, VA 22904*

⁷*Division of Chemistry and Chemical Engineering, California Institute of Technology, Pasadena, CA 91125*

⁸*B.A. McGuire is a Jansky Fellow of the National Radio Astronomy Observatory*

⁹*N. Dollhopf was a summer student at the National Radio Astronomy Observatory*

¹⁰*S.T. Booth was a summer student at the National Radio Astronomy Observatory*

Accepted 8 September 2016

ABSTRACT

Bell et al. (1997) reported the first detection of the cyanopolyne HC₁₁N toward the cold dark cloud TMC-1; no subsequent detections have been reported toward any source. Additional observations of cyanopolyynes and other carbon-chain molecules toward TMC-1 have shown a log-linear trend between molecule size and column density, and in an effort to further explore the underlying chemical processes driving this trend, we have analyzed GBT observations of HC₉N and HC₁₁N toward TMC-1. Although we find an HC₉N column density consistent with previous values, HC₁₁N is not detected and we derive an upper limit column density significantly below that reported in Bell et al. (1997). Using a state-of-the-art chemical model, we have investigated possible explanations of non-linearity in the column density trend. Despite updating the chemical model to better account for ion-dipole interactions, we are not able to explain the non-detection of HC₁₁N, and we interpret this as evidence of previously unknown carbon-chain chemistry. We propose that cyclization reactions may be responsible for the depleted HC₁₁N abundance, and that products of these cyclization reactions should be investigated as candidate interstellar molecules.

Key words: ISM: molecules, ISM: individual objects: TMC-1, Physical Data and Processes, line: identification

1 INTRODUCTION

Carbon chains are the starting point for a significant fraction of the known chemical complexity within the interstellar medium (Thaddeus & McCarthy 2001). In addition to forming the backbone of the polyne families (cyanopolyynes, methylpolyynes, and methylcyanopolyynes) (e.g. Irvine et al. 1981; Bell et al. 1997; Snyder et al. 2006; Remijan et al. 2006), carbenes such as H₂C₅ and H₂C₆ (McCarthy et al. 1997b,a), and unsaturated hydrocarbons such as HC₄H

and HC₆H (Cernicharo et al. 2001), they are also the precursors of a number of interstellar anions (McCarthy et al. 2006; Brünken et al. 2007; Cernicharo et al. 2007; Thaddeus et al. 2008). Additionally, carbon-chain species may play an important role in the formation of polycyclic aromatic hydrocarbons (PAHs) (Tielens 2008; Duley & Hu 2009), and are promising candidates as carriers of the diffuse interstellar bands (Thaddeus 1995; Tulej et al. 1998; Motylewski et al. 2000; Thaddeus & McCarthy 2001; Maier et al. 2004; Jochnowitz & Maier 2008; Zack & Maier 2014). Thus, studying the formation and destruction chemistry of carbon-chain molecules promises to provide insight into a large subset of interstellar chemistry.

* E-mail: rloomis@cfa.harvard.edu

† Deceased

A particularly well-studied family of carbon-chains are the cyanopolyynes: linear molecules of the form HC_nN , where $n = 3, 5, 7, 9, \text{etc.}$ As with the other carbon-chains, cyanopolyynes are observed in high abundance toward asymptotic giant branch (AGB) stars (e.g. [Truong-Bach et al. 1993](#); [Agúndez et al. 2008](#)) and cold dark clouds such as the Taurus molecular cloud (TMC-1) (e.g. [Bujarrabal et al. 1981](#); [Hirahara et al. 1992](#); [Ohishi & Kaifu 1998](#); [Kaifu et al. 2004](#); [Gratier et al. 2016](#)). The polyyne families of molecules in TMC-1 share a surprisingly linear correlation between their log abundances and size ([Bujarrabal et al. 1981](#); [Bell et al. 1997](#); [Ohishi & Kaifu 1998](#); [Remijan et al. 2006](#)), which can be explained by a formation chemistry governed by a small set of gas-phase reactions to add carbons to the chain ([Winnewisser & Walmsley 1979](#); [Bujarrabal et al. 1981](#); [Fukuzawa et al. 1998](#)). Observations of AGB stars such as IRC+10216 and CRL2688 also show abundances of cyanopolyynes that follow the same downward trend (e.g. [Truong-Bach et al. 1993](#)), suggesting that the underlying gas-phase formation mechanisms are similar for both AGB stars and cold cores.

Given this linear trend and assumption of relatively simple chemistry, both laboratory and observational studies have attempted to find larger cyanopolyynes. In the laboratory, cyanopolyne chains up to HC_{17}N have been detected ([McCarthy et al. 1998a](#)), while HC_{11}N is the largest detected interstellar cyanopolyne. Originally thought to be detected in the AGB star IRC+10216 ([Bell et al. 1982](#)), refinements to transition rest frequencies of HC_{11}N brought the detection into dispute ([Travers et al. 1996](#)), and a further search of IRC+10216 yielded a non-detection (M. Bell, unpublished). Utilizing new laboratory data, a deep search of TMC-1 was undertaken by [Bell et al. \(1997\)](#) using the NRAO 140 foot telescope at Green Bank, resulting in a reported detection of two HC_{11}N transitions roughly in agreement with predictions of the linear abundance trend. No subsequent detections of HC_{11}N have been reported toward any astronomical source.

In this paper, we present an analysis of observations originally taken with the intent to confirm the HC_{11}N detection, and to identify HC_{13}N toward TMC-1. We report a non-detection of HC_{11}N in conflict with the column density reported by [Bell et al. \(1997\)](#), and attempt to resolve these discrepant observations. Utilizing a state-of-the-art chemical modeling code, we calculate cyanopolyne abundances in TMC-1 and comment on possible reasons for a depleted abundance of HC_{11}N .

In Section 2 we describe the observations, in Section 3 the observational results are presented, and in Section 4 the observational method is reviewed for possible explanations of the HC_{11}N non-detection. In Section 5 we present our chemical modeling results and compare to the observations, and in Section 6 we summarize our results.

2 OBSERVATIONS

We utilize observations on the Robert C. Byrd Green Bank Telescope (GBT) from project AGBT06A_046 (PI: G. Langston). Extensive details of the observations and calibration are presented in [Langston & Turner \(2007\)](#), and are briefly summarized here. Observations of the TMC-

1 cyanopolyne peak ($4^{\text{h}}41^{\text{m}}42^{\text{s}}$, $25^{\circ}41'27''$ J2000) were taken in Ku-band (11.7 GHz to 15.6 GHz) over 28 epochs in 2006, for a total of ~ 180 hrs integration time. For the first 12 epochs, the GBT spectrometer was configured for dual beam, dual polarization observations with four 12.5 MHz spectral windows. Each 12.5 MHz spectrum consisted of 4096 channels (3052 Hz resolution, 0.070 km s^{-1}). In the remaining 16 epochs, an identical setup was used, but with a larger bandwidth of 50 MHz. Each 50 MHz spectrum consisted of 16384 channels, providing an identical spectral resolution to the previous epochs.

Observations were taken using the “nodding” mode, alternating between the two Ku-band receiver feeds, separated by an angular offset of $330''$ on the sky. This angular separation is sufficiently large such that there is no significant cyanopolyne emission from TMC-1 in the “off” position feed. To confirm correct pointing, the HC_{11}N observations were preceded most days by short test observations of the HC_5N $J=5-4$, HC_7N $J=11-10$, HC_7N $J=12-11$, and HC_9N $J=23-22$ transitions. As reported by [Langston & Turner \(2007\)](#), the observed HC_7N $J=11-10$ intensity was a factor of 2.05 ± 0.05 stronger than the value reported by [Bell et al. \(1997\)](#), suggesting both an accurate pointing as well as a beam filling factor of close to unity for the GBT observations (see Section 4).

Peak and focus observations were performed on the quasar 3C123. The data were reduced using the *rt-idl* and *GBTIDL* packages. Antenna temperatures were recorded on the T_A scale with conservatively-estimated 20% uncertainties, and were then converted to the T_b scale by correcting for the main beam and aperture efficiencies (for a detailed discussion of the antenna temperature calibration, see [Langston & Turner \(2007\)](#)). A systemic velocity of $v_{\text{LSR}} = +5.8 \text{ km s}^{-1}$ was assumed ([Kaifu et al. 2004](#)).

3 OBSERVATIONAL RESULTS

Six consecutive transitions of HC_9N and six consecutive transitions of HC_{11}N were covered by the observations. Rest frequencies for all transitions were obtained from the Splatalogue database²³. We are highly confident in these rest frequencies, as the original HC_{11}N laboratory data span the range of the astronomical observations (6–15 GHz), and the rest frequencies were measured to very high spectral resolution, i.e. $< 0.1 \text{ km s}^{-1}$ ([Travers et al. 1996](#); [McCarthy et al. 1997a](#)). Additionally, ^{13}C and ^{15}N isotopic spectroscopy confirmed the elemental composition and geometry of the molecule ([McCarthy et al. 2000](#)).

All six HC_9N transitions were detected at the systemic velocity of $+5.8 \text{ km s}^{-1}$ (Figure 1), and their intensities and line-widths are reported in Table 1. A column density of $2.3 \pm 0.2 \times 10^{12} \text{ cm}^{-2}$ and rotational temperature of $10 \pm 2 \text{ K}$ were calculated using the formalism described in [Hollis et al. \(2004\)](#), assuming optically thin emission that fills the telescope beam. These values are consistent with previous observations of HC_9N in TMC-1, as are the measured line-widths ([Bell et al. 1997](#); [Kaifu et al. 2004](#); [Kalenskii et al.](#)

² Available at www.splatalogue.net ([Remijan et al. 2007](#)).

³ Frequencies are catalogued through CDMS ([Müller et al. 2001, 2005](#)).

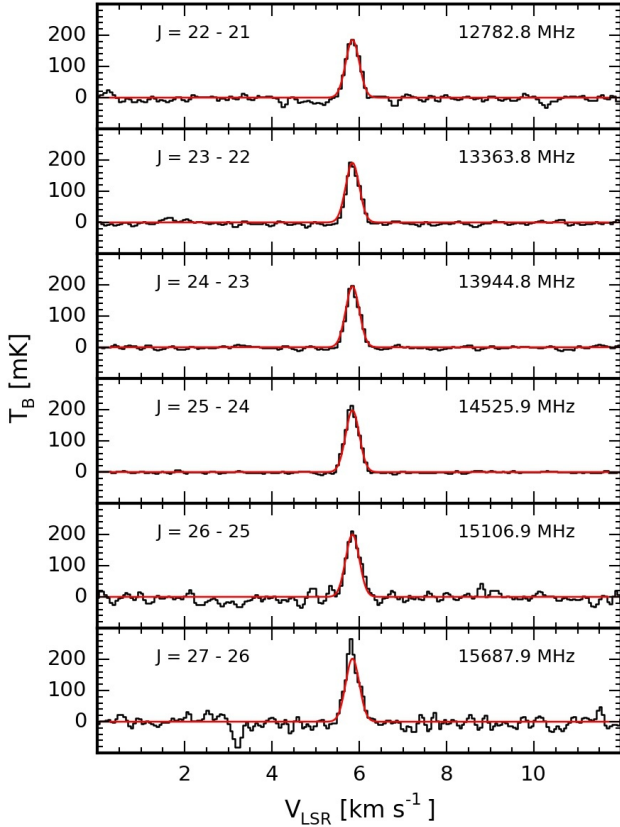


Figure 1. Observations of HC₉N transitions with predictions using the best fit column density and rotational temperature overplot in red.

2004; Remijan et al. 2006). We take this as evidence that there are no large systematic errors with the observations, and that our assumptions about both the beam filling factor and the “off” nodding positions are reasonable (see Section 4).

Our observations of the six HC₁₁N transitions are shown in Figure 2; none were identified above a 2σ significance at $+5.8$ km s⁻¹. All of these transitions were high J (> 30) and a -type ($\mu_a = 5.47(5)$ D) (P. Botschwina, private communication (1997) in Bell et al. (1997)), similar to and including both transitions from Bell et al. (1997). The rms noise of the spectra ranges from 2–3 mK for four of the transitions, and 6–7 mK for the remaining two transitions, which had less integration time. The 3σ noise levels for each respective spectrum are shown as dashed blue lines. Based on the column density reported in the Bell et al. (1997) detection, and the characteristic cyanopolyne properties of TMC-1 (e.g. Kaifu et al. 2004), we over-plot in red a predicted spectrum for each transition, using a line width of 0.4 km s⁻¹ and excitation temperature of 10 K (Bell et al. 1997). These predicted spectra take into account the different beam filling factor of the cyanopolyne emission region for the GBT and the NRAO 140ft telescope (see Section 5.1). The predicted intensities range from 11–13 mK, equivalent to a 4–5 σ signal in the higher SNR spectra, but we do not observe any signals of this strength.

To further constrain the abundance of HC₁₁N, we

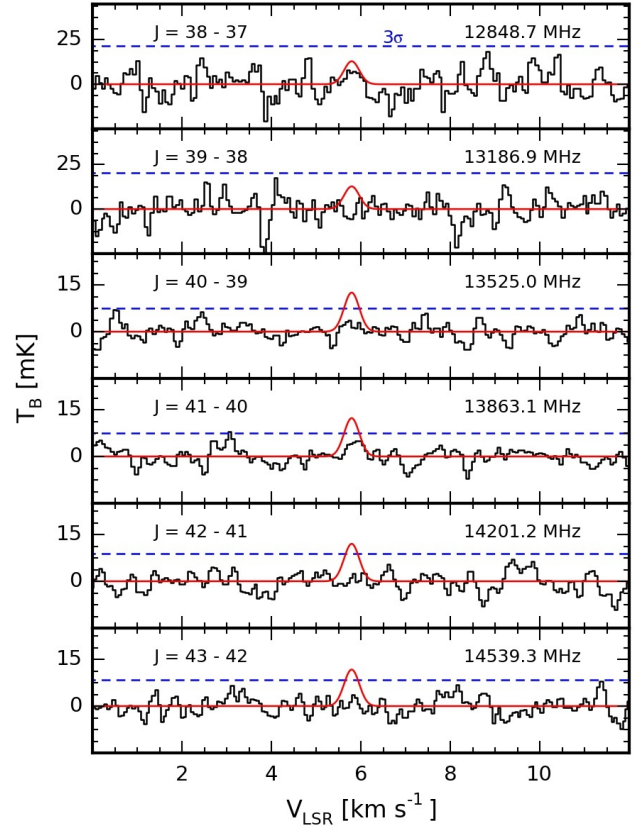


Figure 2. Observations of HC₁₁N rest frequencies with overplot of predictions from the Bell et al. (1997) column density in red. The 3σ noise level for each spectrum is shown in blue.

weighted the spectra by their variances and stacked them, shown in Figure 3. Spectral stacking is particularly well suited for the linear cyanopolyynes (e.g. Langston & Turner 2007), which have regular and well characterized transition rest frequencies and smoothly varying intensities (e.g. Figure 1 and Table 1 for HC₉N). At an excitation temperature of 10 K, our predicted intensities only change by $\sim 15\%$ from the least to most energetic observed transition. As noted by Bell et al. (1998) and Ohishi & Kaifu (1998), however, radiative cooling likely plays an important role in determining the cyanopolyne excitation temperatures in TMC-1, with the smaller cyanopolyynes being more affected. Due to its size, HC₁₁N should be less affected, and Bell et al. (1998) predicts an excitation temperature of 8–10 K. Even at a pessimistic excitation temperature of 5 K, however, our predicted intensities would only change by $\sim 33\%$ from the least to most energetic observed transition. Thus we believe that spectral stacking is a valid method for placing limits on HC₁₁N emission. The stacked HC₁₁N spectrum has an rms of 1.4 mK, and we observe no signal in excess of 2σ at $+5.8$ km s⁻¹.

To quantitatively characterize an upper limit on the HC₁₁N column density, we used a Markov chain Monte Carlo (MCMC) code (Foreman-Mackey et al. 2013) to generate posterior probability distributions of the brightness temperature in each spectrum. The probability density function describes the range of possible brightness temperatures that are consistent with our observed data. As seen in Figure 2,

Table 1. Observed transitions of HC₉N and HC₁₁N upper limits

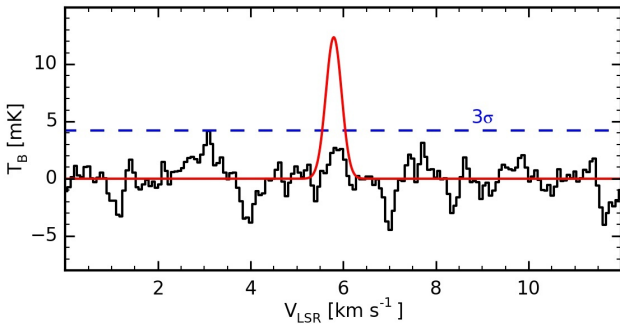
HC ₉ N					
Transition J' – J''	Frequency ^{ab} (MHz)	E _u (K)	S _{ij} μ ² (D ²)	ΔT _b (mK)	ΔV (km s ⁻¹)
22 – 21	12782.8	7.05	595	189(6)	0.37(2)
23 – 22	13363.8	7.70	622	188(4)	0.35(1)
24 – 23	13944.8	8.37	649	191(2)	0.36(1)
25 – 24	14525.9	9.06	676	201(2)	0.39(1)
26 – 25	15106.9	9.79	703	201(9)	0.38(2)
27 – 26	15687.9	10.54	730	226(11)	0.39(2)

HC ₁₁ N					
Transition J' – J''	Frequency ^{ab} (MHz)	E _u (K)	S _{ij} μ ² (D ²)	ΔT _b ^c (mK)	Column Density (10 ¹¹ cm ⁻²)
38 – 37	12848.7	12.02	1137	< 18.3	< 4.1
39 – 38	13186.9	12.66	1167	< 6.8	< 1.5
40 – 39	13525.0	13.31	1197	< 6.8	< 1.5
41 – 40	13863.1	13.97	1227	< 8.6	< 2.0
42 – 41	14201.2	14.65	1256	< 4.9	< 1.1
43 – 42	14539.3	15.35	1287	< 5.2	< 1.2

^a Beam sizes and efficiencies for each respective frequency can be found in [Hollis et al. \(2007\)](#).

^b Rest frequencies were obtained from the Splatalogue database, see Sect. 3 for complete references.

^c Brightness temperature upper limits are the 95% confidence level values derived for each respective spectrum.

**Figure 3.** Weighted stacked spectra, with overplot of predictions from the [Bell et al. \(1997\)](#) column density in red. The 3σ noise level is shown in blue.

the noise in the spectra are heavily correlated, due to the weighted convolution kernel used in re-gridding the spectra to correct for frequency smearing from Doppler tracking (see Section 2.3 of [Langston & Turner 2007](#)). Thus, our calculated rms values for each spectrum are insufficient to describe the uncertainties in the data. To properly account for this correlation in the noise, we use a Gaussian Process Regression code⁴ ([Ambikasaran et al. 2014](#)) to construct a noise covariance matrix with a Matérn 3/2 kernel. This approach more accurately describes our uncertainties, resulting in a larger, but more realistic upper limit. From these fits, we report the 95% confidence level brightness temperature upper

limits of each transition and their respective column density limits in Table 1. Column density upper limits were calculated using the formalism described in [Hollis et al. \(2004\)](#), assuming optically thin emission, a rotational temperature of 10 K, and our measured HC₉N line-width of 0.37 km s⁻¹.

Combining all of the spectral fits, we generate the total posterior probability distribution for column density, shown in Figure 4. As there is no clear detection of signal, the posterior is only useful in generating an upper limit, and we can exclude at a 95% confidence level a column density greater than $\sim 9.4 \times 10^{10}$ cm⁻². Also shown in Figure 4 are the column density calculated from our chemical model (see Section 5), and the column density reported by [Bell et al. \(1997\)](#). To determine the compatibility of our results with those of [Bell et al. \(1997\)](#), we have additionally plotted a probability distribution for the [Bell et al. \(1997\)](#) column density, calculated using the errors reported for their two detected line intensities. As seen in the figure, there is essentially no overlap between the two probability distributions. We therefore conclude that our observations are in disagreement with those of [Bell et al. \(1997\)](#).

In Figure 5, we plot our measured HC₉N and upper limit HC₁₁N column densities with literature cyanopolyne column densities toward TMC-1 ([Bell et al. 1997](#); [Kaifu et al. 2004](#); [Kalenskii et al. 2004](#); [Remijan et al. 2006](#); [Langston & Turner 2007](#); [Cordiner et al. 2013](#)). Only one recent value is shown for the optically thick species HC₃N, as many literature HC₃N column densities are calculated assuming optically thin emission and are artificially low. From these literature column densities, we have calculated a best fit linear trend, plotted as a black dashed line. Our observed HC₉N column density is in good agreement with this trend, but

⁴ available at <https://github.com/dfm/george>

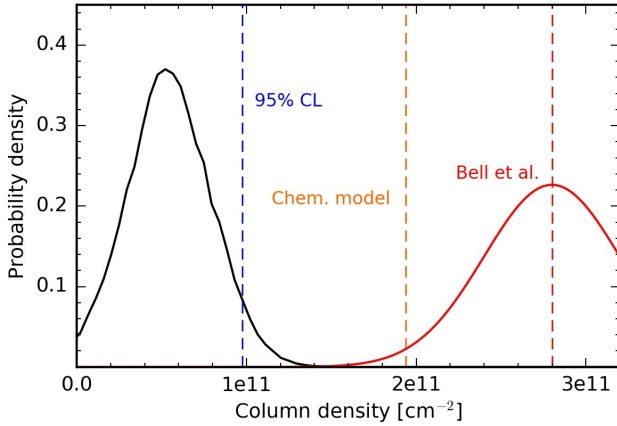


Figure 4. Posterior probability distribution of HC_{11}N column density derived from our MCMC fits to the individual spectra. The column density derived in Bell et al. (1997) and the predicted column density from our chemical model are also shown for comparison.

our upper limit for HC_{11}N significantly deviates both from the Bell et al. (1997) observations and the trend, suggesting additional cyanopolyne chemistry at sizes larger than HC_9N .

4 POSSIBILITY OF SYSTEMATIC ERRORS

We have shown that HC_{11}N emission is absent from the present GBT observations, in conflict with the column density reported by Bell et al. (1997). It is possible, however, that our analysis of the GBT observations is flawed due to systematic errors in either the reduced data or in our assumptions. Here we investigate four possible sources of error in our analysis: contamination in the “off” position during the nodding observations, an inaccurate assumption of the beam filling factor, antenna temperature calibration uncertainties, and the validity of an LTE analysis.

4.1 “Off” position contamination

The GBT observations were taken in a nodding mode, and in the data reduction the “off” position data were subtracted from the “on” position data. Any molecular emission from the “off” position would weaken the measured line strengths, possibly dramatically decreasing their intensity. This is especially a concern in an extended source such as TMC-1, as the angular offset of the two beams of the Ku-band receiver is relatively small ($330''$). While TMC-1 extends over $10'$ along its principal axis, cyanopolyne emission arises from a more compact region, spanning roughly $6.0' \times 1.3'$ (Churchwell et al. 1978; Olano et al. 1988; Bell et al. 1997). Our $5.5'$ nodding offset is then likely sufficient to prevent contamination, placing the “off” beam a safe distance away from the emission region. By examining the raw “on” and “off” spectra for HC_9N (taken simultaneously with the HC_{11}N spectra) and assuming that HC_9N would trace the same emission region as HC_{11}N , we are able to rule out this possible source of systematic error (Figure 6).

4.2 Beam filling factor

The NRAO 140 ft telescope and the GBT have beams that differ in size by approximately a factor of 2 at a given frequency. Comparison of derived column densities therefore rests upon an accurate assessment of the beam filling factor of the source emission region. In their column density calculation, Bell et al. (1997) assume that all cyanopolyne emission arises from the previously mentioned $6.0' \times 1.3'$ region, yielding a beam-filling factor of 0.54 for their $2.4'$ beam. The mapping results of Hirahara et al. (1992), Pratap et al. (1997), and Fossé et al. (2001) show that HC_3N emission traces a region approximately this size and shape, confirming that the Bell et al. (1997) beam-filling factor estimate is reasonable. We can then safely assume that the $1.2'$ GBT beam is completely filled.

4.3 Antenna temperature calibration

The antenna temperatures for our observations were calibrated using noise diodes (see Langston & Turner (2007) for details), while those from Bell et al. (1997) were recorded on the T_A^* scale, presumably calibrated using a chopper wheel (e.g. Ulich & Haas 1976). Antenna temperature calibration uncertainty is often reported at levels of 10 – 30%, and might possibly introduce a relative bias between the two measurements. Although we cannot directly constrain the relative uncertainty due to either the antenna temperature calibration or beam filling factor assumptions, we can quantify the uncertainty in derived column densities, which is the compared quantity between the two observations.

For optically thin lines, a bias in antenna temperature will correspond linearly to a bias in derived column density, as would a change in the beam filling factor assumption. Since the smaller cyanopolyne lines have numerous observations (e.g. Bell et al. 1997; Kalenskii et al. 2004; Remijan et al. 2006; Langston & Turner 2007), we can use the scatter in the derived column densities to estimate how biased a given set of observations might be. Without including the results of Bell et al. (1997), the scatter for the HC_5N , HC_7N , and HC_9N column densities shown in Figure 5 is 9%. Including the Bell et al. (1997) column densities brings this scatter to 16%, as they are slightly systematically low compared to literature averages. The column densities reported here and in Langston & Turner (2007) are well within this scatter, suggesting that there is unlikely to be a greater than $\sim 20\%$ column density bias between our observations and Bell et al. (1997). As Bell et al. (1997) column densities are systematically low, this might signify a small error in either their antenna temperature calibration or assumed beam filling factor. If this was to be corrected, however, it would increase their HC_{11}N column density and create more conflict between the two datasets. Even so, to be conservative we compare our derived column density with that of Bell et al. (1997) shifted down by 20%, and we find a $<1\%$ chance that the two datasets are compatible. We additionally note that our derived $\text{HC}_9\text{N}/\text{HC}_{11}\text{N}$ ratio is quite different from that of Bell et al. (1997) (>24 vs 6.8), which should be independent of any absolute calibration uncertainty. Thus we conclude that uncertainties in calibration or beam filling factor are unlikely to be able to explain discrepancies between the two sets of observations.

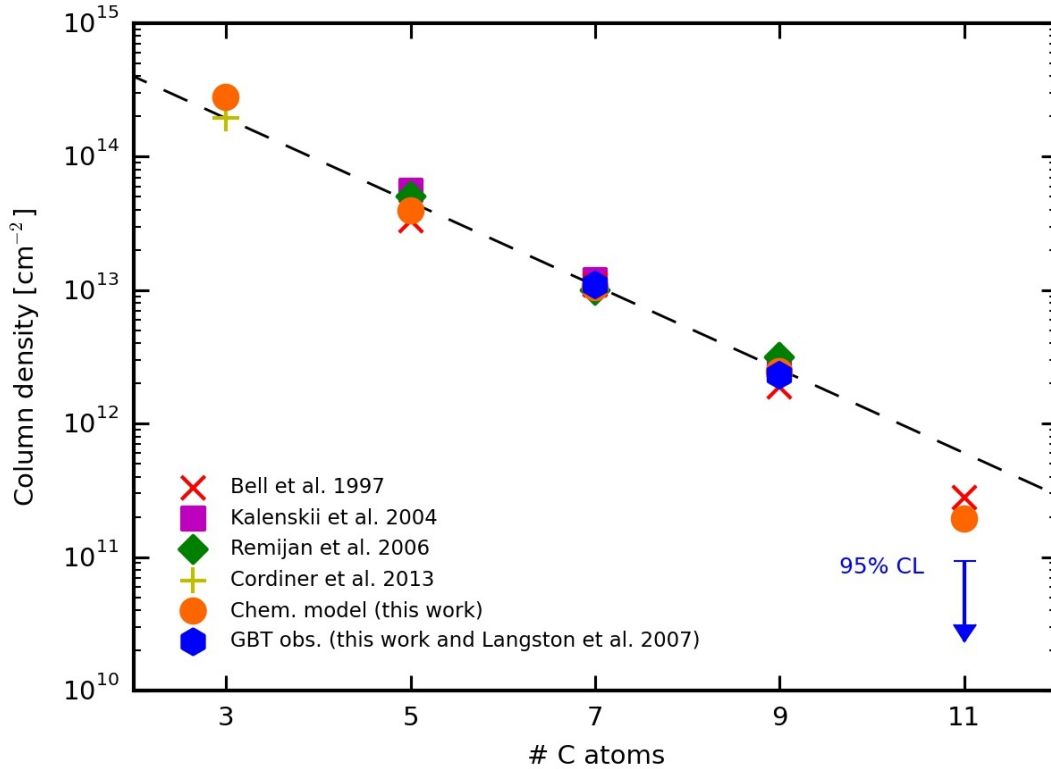


Figure 5. Cyanopolyne column densities from the literature, along with our observations and chemical modeling results.

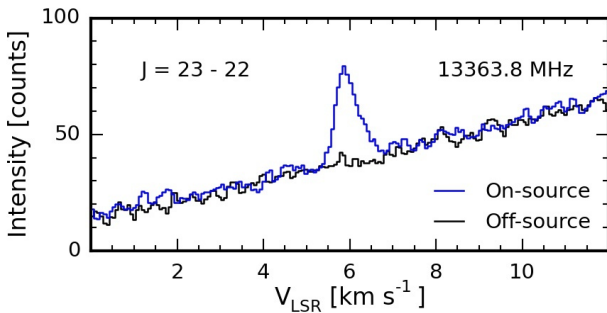


Figure 6. Raw on-source and off-source nodding spectra of the HC_9N $J=23-22$ transition, shown in blue and black respectively. As there is no “off” source to calibrate the “off” data against, an intensity unit of counts is used, and a scalar value is subtracted from the “on” data to align them. No HC_9N emission is observed in the off-source spectrum.

4.4 Validity of LTE

In our line strength predictions and calculations of column densities we have assumed LTE excitation of the cyanopolyynes in TMC-1, as was assumed in Bell et al. (1997, 1998); Ohishi & Kaifu (1998); Kaifu et al. (2004); Langston & Turner (2007). The critical densities of HC_9N and HC_{11}N are not well known, as their collisional cross-sections have not been measured, but can be estimated by scaling the cross section of HC_3N (Green & Chapman 1978; Avery et al. 1979; Snell et al. 1981). The change to the cross-

section is estimated as a linear scaling proportional to the size of the molecule, yielding an HC_{11}N cross section $\sim 3\times$ larger than that of HC_3N . In reality, the cross section is likely significantly larger, but the linear scaling provides a good upper limit estimate of the critical density. From this scaled cross-section ($\sim 3\times 10^{-14}\text{cm}^2$), an assumption of a kinetic gas temperature of 10K, and A_{ij} values from the Splatalogue database, we estimate a critical density between 300 and 800 cm^{-3} for the HC_{11}N transitions covered by our observations. Similarly, we estimate a critical density between 400 and 900 cm^{-3} for our observed HC_9N transitions. These critical densities are significantly smaller than the gas density of TMC-1, $2\times 10^4\text{cm}^{-3}$ (Liszt & Ziurys 2012; Hincelin et al. 2011), suggesting that the observed transitions are fully thermalized and our assumption of LTE is reasonable. Future work on the collisional cross sections of larger cyanopolyynes may allow for more detailed statistical equilibrium calculations and a more careful analysis of the observed linear abundance trend in cyanopolyne column densities.

4.5 Possible correlator artifacts

Finally, we turn to the possibility that the Bell et al. (1997) observations are spurious. The HC_{11}N features observed by Bell et al. (1997) could be attributed to frequency switching artifacts from the correlator, which they mention as a possible explanation for several nearby U-lines. The small-offset frequency switching method used by Bell et al. (1997) in particular may be susceptible to this problem; telluric lines and local interference can be removed using a short off-source integration, but this would not remove the effects

of weak correlator artifacts (Bell & Feldman 1991; Bell et al. 1993). Bell et al. (1997) mention that they utilize two sets of observations with HC₁₁N in different filter banks to reduce these effects, but it is unclear how effective this is, especially in conjunction with their LINECLEAN method of removing frequency-switched images (Bell 1997). We do not observe U-lines of similar intensity in our position switched data (Figures 1 and 2), and no known molecular lines correspond to the U-lines recorded in Bell et al. (1997). Additionally, the noise in the Bell et al. (1997) spectra is correlated on roughly similar scales to the characteristic line-width of TMC-1 (0.4 km s⁻¹), which could explain their observed line-widths if the HC₁₁N features and U-lines were artifacts.

In short, we are confident in the quality of the observations presented here and in Langston & Turner (2007), as our measured column densities agree quite well with previous observations. We are therefore also confident in our non-detection of HC₁₁N in this dataset, and the derived HC₉N/HC₁₁N column density ratio that contradicts the previously suggested log-linear abundance trend (Remijan et al. 2006). Although our analysis suggests that our observations are in conflict with those of Bell et al. (1997), we can not conclusively show whether this is due to measurement and calibration errors, or whether the Bell et al. (1997) detection is spurious. In either case, the deviation of the HC₁₁N abundance from the log-linear trend requires further chemical investigation.

5 CHEMICAL MODELING

5.1 Modeling code and updated reactions

As shown in Figure 5, our observations in combination with literature values suggest that although the smaller cyanopolyynes have a log-linear abundance trend, HC₁₁N is clearly an outlier. To investigate possible chemical explanations of this, we have modeled the chemistry of HC₁₁N and other smaller cyanopolyynes in TMC-1. We used the deterministic gas-grain rate equation model Nautilus (Druard & Wakelam 2012) with the 2014 KIDA network of chemical reactions (Wakelam et al. 2012, 2015), updated to include reactions for HC₁₁N and several related species (see Table 2 and the online supplementary data). The physical conditions used in the model were chosen to be representative of TMC-1, i.e. a kinetic temperature of 10 K and a gas density of 2×10^4 cm⁻³, as were the initial elemental abundances (Liszt & Ziurys 2012; Hincelin et al. 2011).

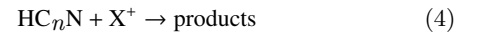
In the model, our added reactions for HC₁₁N follow those of the smaller cyanopolyynes included in the network. The formation chemistry of cyanopolyynes and other unsaturated carbon-chain species is dominated by gas-phase reactions. Grain-surface contributions are negligible, as unsaturated carbon chains rapidly react with hydrogen on grain surfaces, producing saturated hydrocarbons. Unsaturated carbon-chain molecules are often formed via reactions between smaller carbon-chains through the addition of one or more carbons to the backbone. One such reaction, which is a major formation route for cyanopolyynes (Fukuzawa et al. 1998), is



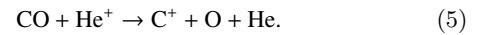
Cyanopolyynes can also form via reactions involving precursors with the same number of carbons, two important examples of which are:



Finally, the destruction of cyanopolyynes is dominated by reactions with ionic species. These have the general form



where X⁺ is some ionic species, e.g. C⁺, H⁺, H₃⁺, or HCO⁺. Ionized carbon is a particularly important co-reactant in many of the destruction pathways, and is formed in the model mainly via the dissociation of CO by cosmic-ray ionized helium (Rimmer et al. 2012), i.e.



The rate coefficients for most reactions in the code are calculated using the Arrhenius-Kooij formula,

$$k(T) = \alpha \left(\frac{T}{300 \text{ K}} \right)^\beta \exp^{-\gamma/T} \quad (6)$$

where α is a temperature independent pre-exponential factor, β governs the temperature dependence, and γ is the energy barrier. Many of the reactions are difficult, if not impossible, to study in the laboratory. Thus in the absence of experimental values, rate coefficients were estimated via extrapolation from similar reactions involving smaller carbon-chain species or via a standard formula such as the Langevin rate for ion-dipole reactions. Our added reactions and their corresponding values of α , β , and γ are listed in Table 2.

5.2 Ion-dipole effects

Reactions between ions and neutral molecules with a dipole moment are often both barrier-less and inversely temperature dependent, i.e. $\gamma = 0$ and $\beta < 0$ (Clary 2008), meaning that they are particularly efficient in cold regions such as TMC-1. The rate coefficients for these reactions are proportional to the dipole moment of the neutral reactant molecule, and the 2014 KIDA network has the advantage of accounting for this phenomenon.

For the reactions mentioned above, the rate coefficients will increase with cyanopolyne length, due to the enhancing effect of both a larger physical cross-section and dipole moment. For example, the ratio of rate coefficients for the destruction reactions of HC₁₁N and HC₃N with the ion HCO⁺, $k_{\text{HC}_{11}\text{N}}/k_{\text{HC}_3\text{N}}$, is ~ 4.75 . Thus larger species, though less abundant, are more reactive. This should add a small non-linear contribution to the cyanopolyne abundance trend, which will become more pronounced in larger molecules such as HC₁₁N.

Table 2. Reactions Added to Network^a

Reaction	α^b	β^b	γ^b
$\text{HC}_{11}\text{N} + \text{photon} \rightarrow \text{C}_{11}\text{HN}^+ + \text{e}^-$	2.0×10^{-10}	0.0	2.5
$\text{CN} + \text{C}_{10}\text{H}_2 \rightarrow \text{H} + \text{HC}_{11}\text{N}$	2.7×10^{-10}	-0.5	19
$\text{HC}_{11}\text{N} + \text{H}^+ \rightarrow \text{H} + \text{C}_{11}\text{HN}^+$	4.9×10^{-08}	-0.5	0
$\text{HC}_{11}\text{N} + \text{H}_3^+ \rightarrow \text{H}_2 + \text{C}_{11}\text{H}_2\text{N}^+$	2.7×10^{-08}	-0.5	0
$\text{HC}_{11}\text{N} + \text{HCO}^+ \rightarrow \text{CO} + \text{C}_{11}\text{H}_2\text{N}^+$	1.7×10^{-08}	-0.5	0

^a Table 2 is published in its entirety in the electronic edition of *MNRAS*. A portion is shown here for guidance regarding its form and contents.

^b Parameter units depend on the type of reaction and rate-coefficient formula

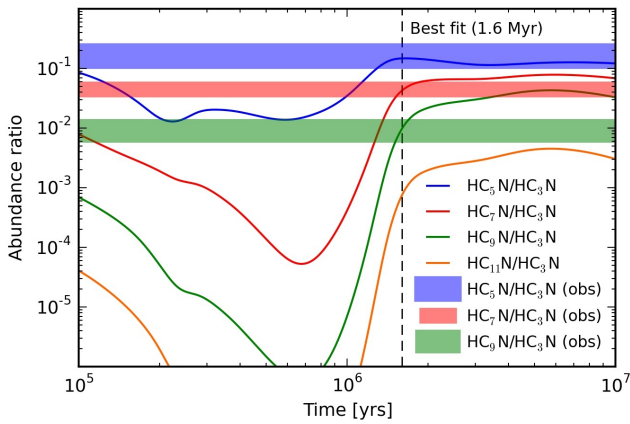


Figure 7. Ratios of cyanopolyne abundances in our chemical model, with observational column density ratios overplotted. The spread in each observational column density ratio is shown by the width of the line.

5.3 Comparison of model results and observations

The chemical model was run to a final time of 10 Myr, and we derive a best fit time of ~ 1.6 Myr by comparing cyanopolyne abundance ratios from literature averages and the model (Figure 7). This age is similar to previous estimates of the chemical age of TMC-1 (Brown & Charnley 1990; Ruffle & Herbst 2001). The chemical model abundances from 1.6 Myr are given in Table 3. To scale these abundances to column densities, we fit a proton column density of $1.3 \times 10^{23} \text{ cm}^{-2}$. Assuming that molecular hydrogen is the dominant proton carrier, this roughly corresponds to a molecular hydrogen column density of $7 \times 10^{22} \text{ cm}^{-2}$, within an order of magnitude of other estimates (Suutarinen et al. 2011). For HC_{11}N , the predicted abundance relative to the proton density is 1.4×10^{-12} , yielding a column density of $1.9 \times 10^{11} \text{ cm}^{-2}$. While this column density falls below the predicted linear trend (Remijan et al. 2006) and the observed value of $2.8 \times 10^{11} \text{ cm}^{-2}$ (Bell et al. 1997), it is still above our 95% confidence level upper limit column density of $9.4 \times 10^{10} \text{ cm}^{-2}$ (Figures 4 & 5). Thus, although the additional consideration of ion-dipole effects in our modeling relieves some tension with the data by introducing a non-linear contribution to the abundance trend, there may be additional chemistry unaccounted for by the model.

6 DISCUSSION

As suggested by Bell et al. (1997) and Remijan et al. (2006), it has been previously assumed that the chemistry of long (>10 atoms) carbon-chain species would follow the general pattern of the smaller ones, and that it should be possible to detect not only HC_{11}N , but HC_{13}N as well. This is the basic assumption behind the added HC_{11}N reactions in our chemical model. Our observations, however, suggest additional chemistry for cyanopolynes, and possibly other carbon-chain species, larger than HC_9N .

Our low upper limit on the abundance of HC_{11}N suggests that there may be an unknown destruction mechanism for either HC_{11}N or one of its precursors, such as $\text{C}_{11}\text{H}_2\text{N}^+$. Although destruction through reaction with ions is considered in our chemical model, isomerization reactions such as cyclization were not included. Cyclization of large cyanopolynes may be supported by studies of pure carbon clusters, i.e. C_n , which are analogous to cyanopolynes in their carbon-chain structure (see review article by Weltner & Van Zee (1990)). Experiments show that carbon clusters up to 9 atoms exist mainly in a linear form, while 10 atom clusters are a mixture of linear and monocyclic isomers, and clusters of 11 or more atoms exist purely as cyclic structures (von Helden et al. 1993). This behavior is easily understood, as cyclic isomers become more thermodynamically stable than their linear counterparts at larger sizes (Van Orden & Saykally 1998). Additionally, at larger sizes the number of possible isomers rapidly increases and the barriers to isomerization reactions shrink, making spontaneous isomerization more likely. These properties should generally extrapolate from carbon clusters to cyanopolynes, and thus at sizes larger than 11 atoms (i.e. larger than HC_9N), the cyclic forms of long carbon-chains could become a “sink”, depleting abundances of linear forms (Travers et al. 1996; McCarthy et al. 2000).

The products of this isomerization would depend on the parent species, and might contain both cyclic and linear components, resembling known ring-chain molecules such as C_7H_2 , C_9H_2 , HC_4N , and HC_6N (McCarthy et al. 1997c, 1998b, 1999). None of these molecules have yet been found in their ring-chain forms toward interstellar sources (Cernicharo et al. 2004), but this may be related to their small size, as the cyclization reactions would be more prevalent for the larger polynes. Our observations suggest that more laboratory work should be conducted to investigate the rotational spectra of larger ring-chain species, and that system-

Table 3. Cyanopolyynes abundances and calculated column densities

Molecule	Abundance ^a Chemical Model ($\times 10^{-12}$)	Column Density ^b Chemical Model ($\times 10^{11}$ cm ⁻²)	Column Density ^c Observations ($\times 10^{11}$ cm ⁻²)
HC ₃ N	2060	2770	1950
HC ₅ N	291	392	452
HC ₇ N	78	105	110
HC ₉ N	18	25	25
HC ₁₁ N	1.4	1.9	2.8 ^d

^a Relative to the proton density, $n_p = n_H + 2n_{H_2}$.^b Calculated from chemical model abundances assuming $n_{H_2} = 7 \times 10^{22}$ cm⁻².^c Calculated from average of all literature measurements presented in Figure 5 (see Section 3).^d Observed column density from Bell et al. (1997). Our 95% confidence level upper limit column density is 9.4×10^{10} cm⁻².

atic searches in survey data toward TMC-1 or IRC-10216 may prove fruitful. Other sources which might host these molecules are the “carbon-chain-producing regions” such as Lupus-1A (Hirota & Yamamoto 2006; Hirota et al. 2009; Sakai et al. 2010).

7 SUMMARY

The results of our analysis of GBT observations of cyanopolyynes toward TMC-1 can be summarized as follows:

- (i) Six transitions of HC₉N were detected; we derive a column density of $2.3 \pm 0.2 \times 10^{12}$ cm⁻² and a rotational temperature of 10 ± 2 K, consistent with previous measurements.
- (ii) Six transitions of HC₁₁N were covered by the observations, but none were detected above 2σ significance.
- (iii) We place a 95% confidence level upper limit on the HC₁₁N column density of 9.4×10^{10} cm⁻², in conflict with the Bell et al. (1997) reported column density of 2.8×10^{11} cm⁻². This is also a significant deviation from previous predictions of a log-linear trend in cyanopolyne abundances.
- (iv) Our chemical model produces a depleted HC₁₁N abundance when the effects of ion-dipole enhancement are included, but is still not able to reproduce the observed upper limit column density.
- (v) Supported by studies of carbon clusters, cyclization reactions may play a role in the depletion of HC₁₁N. The products of these reactions should be pursued as candidate interstellar molecules in future laboratory and astronomical studies.

ACKNOWLEDGEMENTS

We would like to thank M. McCarthy, A. Vanderburg, and B. Montet for productive discussion and helpful comments on the manuscript. We thank two anonymous referees for providing comments that greatly improved the quality of the manuscript. RAL gratefully acknowledges support from a National Science Foundation Graduate Research Fellowship. CNS wishes to thank the National Science Foundation for supporting the Astrochemistry program at the University of

Virginia. BAM and PBC are grateful to G. A. Blake for his support. The National Radio Astronomy Observatory is a facility of the National Science Foundation operated under cooperative agreement by Associated Universities, Inc.

REFERENCES

- Agúndez M., Fonfría J. P., Cernicharo J., Pardo J. R., Guélin M., 2008, *A&A*, **479**, 493
- Ambikasaran S., Foreman-Mackey D., Greengard L., Hogg D. W., O’Neil M., 2014
- Avery L. W., Oka T., Broten N. W., MacLeod J. M., 1979, *ApJ*, **231**, 48
- Bell M. B., 1997, *PASP*, **109**, 609
- Bell M. B., Feldman P. A., 1991, *ApJ*, **367**, L33
- Bell M. B., Feldman P. A., Kwok S., Matthews H. E., 1982, *Nature*, **295**, 389
- Bell M. B., Avery L. W., Watson J. K. G., 1993, *ApJS*, **86**, 211
- Bell M. B., Feldman P. A., Travers M. J., McCarthy M. C., Gottlieb C. A., Thaddeus P., 1997, *ApJ*, **483**, L61
- Bell M. B., Watson J. K. G., Feldman P. A., Travers M. J., 1998, *ApJ*, **508**, 286
- Brown P. D., Charnley S. B., 1990, *MNRAS*, **244**, 432
- Brünken S., Gupta H., Gottlieb C. A., McCarthy M. C., Thaddeus P., 2007, *ApJ*, **664**, L43
- Bujarrabal V., Guélin M., Morris M., Thaddeus P., 1981, *A&A*, **99**, 239
- Cernicharo J., Heras A. M., Tielens A. G. G. M., Pardo J. R., Herpin F., Guélin M., Waters L. B. F. M., 2001, *ApJ*, **546**, L123
- Cernicharo J., Guélin M., Pardo J. R., 2004, *ApJ*, **615**, L145
- Cernicharo J., Guélin M., Agúndez M., Kawaguchi K., McCarthy M., Thaddeus P., 2007, *A&A*, **467**, L37
- Churchwell E., Winnewisser G., Walmsley C. M., 1978, *A&A*, **67**, 139
- Clary D. C., 2008, *Proceedings of the National Academy of Science*, **105**, 12649
- Cordiner M. A., Buckle J. V., Wirstrom E. S., Olofsson A. O. H., Charnley S. B., 2013, *ApJ*, **770**, 48
- Druard C., Wakelam V., 2012, *MNRAS*, **426**, 354
- Duley W. W., Hu A., 2009, *ApJ*, **698**, 808
- Foreman-Mackey D., Hogg D. W., Lang D., Goodman J., 2013, *PASP*, **125**, 306
- Fossé D., Cernicharo J., Gerin M., Cox P., 2001, *ApJ*, **552**, 168
- Fukuzawa K., Osamura Y., Schaefer III H. F., 1998, *ApJ*, **505**, 278

- Gratier P., Majumdar L., Ohishi M., Roueff E., Loison J. C., Hickson K. M., Wakelam V., 2016, *The Astrophysical Journal Supplement Series*, 225, 25
- Green S., Chapman S., 1978, *ApJS*, 37, 169
- Hincelin U., Wakelam V., Guilloteau S., Loison J., Honvault P., Troe J., 2011, *A&A*, 530, A61
- Hirahara Y., et al., 1992, *ApJ*, 394, 539
- Hirota T., Yamamoto S., 2006, *ApJ*, 646, 258
- Hirota T., Ohishi M., Yamamoto S., 2009, *ApJ*, 699, 585
- Hollis J. M., Jewell P. R., Lovas F. J., Remijan A., 2004, *ApJ*, 613, L45
- Hollis J. M., Jewell P. R., Remijan A. J., Lovas F. J., 2007, *ApJ*, 660, L125
- Irvine W. M., Hoglund B., Friberg P., Askne J., Ellender J., 1981, *ApJ*, 248, L113
- Jochnowitz E. B., Maier J. P., 2008, in Kwok S., Sanford S., eds, *IAU Symposium Vol. 251*, IAU Symposium. pp 395–402, doi:10.1017/S1743921308022035
- Kaifu N., et al., 2004, *PASJ*, 56, 69
- Kalenskii S. V., Slysh V. I., Goldsmith P. F., Johansson L. E. B., 2004, *ApJ*, 610, 329
- Langston G., Turner B., 2007, *ApJ*, 658, 455
- Liszt H. S., Ziurys L. M., 2012, *ApJ*, 747, 55
- Maier J. P., Walker G. A. H., Bohlender D. A., 2004, *ApJ*, 602, 286
- McCarthy M. C., Travers M. J., Kovács A., Gottlieb C. A., Thaddeus P., 1997a, *ApJS*, 113, 105
- McCarthy M. C., Travers M. J., Kovacs A., Chen W., Novick S. E., Gottlieb C. A., Thaddeus P., 1997b, *Science*, 275, 518
- McCarthy M. C., Travers M. J., Gottlieb C. A., Thaddeus P., 1997c, *ApJ*, 483, L139
- McCarthy M. C., Grabow J.-U., Travers M. J., Chen W., Gottlieb C. A., Thaddeus P., 1998a, *ApJ*, 494, L231
- McCarthy M. C., Travers M. J., Chen W., Gottlieb C. A., Thaddeus P., 1998b, *ApJ*, 498, L89
- McCarthy M. C., Grabow J.-U., Travers M. J., Chen W., Gottlieb C. A., Thaddeus P., 1999, *ApJ*, 513, 305
- McCarthy M. C., Levine E. S., Apponi A. J., Thaddeus P., 2000, *Journal of Molecular Spectroscopy*, 203, 75
- McCarthy M. C., Gottlieb C. A., Gupta H., Thaddeus P., 2006, *ApJ*, 652, L141
- Motylewski T., et al., 2000, *ApJ*, 531, 312
- Müller H. S. P., Thorwirth S., Roth D. A., Winnewisser G., 2001, *A&A*, 370, L49
- Müller H. S. P., Schlöder F., Stutzki J., Winnewisser G., 2005, *Journal of Molecular Structure*, 742, 215
- Ohishi M., Kaifu N., 1998, *Faraday Discussions*, 109, 205
- Olano C. A., Walmsley C. M., Wilson T. L., 1988, *A&A*, 196, 194
- Pratap P., Dickens J. E., Snell R. L., Miralles M. P., Bergin E. A., Irvine W. M., Schloerb F. P., 1997, *ApJ*, 486, 862
- Remijan A. J., Hollis J. M., Snyder L. E., Jewell P. R., Lovas F. J., 2006, *ApJ*, 643, L37
- Remijan A. J., Markwick-Kemper A., ALMA Working Group on Spectral Line Frequencies 2007, in *American Astronomical Society Meeting Abstracts*. p. 132.11
- Rimmer P. B., Herbst E., Morata O., Roueff E., 2012, *A&A*, 537, A7
- Ruffle D. P., Herbst E., 2001, *MNRAS*, 322, 770
- Sakai N., Shiino T., Hirota T., Sakai T., Yamamoto S., 2010, *ApJ*, 718, L49
- Snell R. L., Schloerb F. P., Young J. S., Hjalmarson A., Friberg P., 1981, *ApJ*, 244, 45
- Snyder L. E., Hollis J. M., Jewell P. R., Lovas F. J., Remijan A., 2006, *ApJ*, 647, 412
- Suutarinen A., et al., 2011, *A&A*, 531, A121
- Thaddeus P., 1995, in Tielens A. G. G. M., Snow T. P., eds, *Astrophysics and Space Science Library Vol. 202*, The Diffuse Interstellar Bands. p. 369
- Thaddeus P., McCarthy M. C., 2001, *Spectrochimica Acta Part A: Molecular Spectroscopy*, 57, 757
- Thaddeus P., Gottlieb C. A., Gupta H., Brünken S., McCarthy M. C., Agúndez M., Guélin M., Cernicharo J., 2008, *ApJ*, 677, 1132
- Tielens A. G. G. M., 2008, *ARA&A*, 46, 289
- Travers M. J., McCarthy M. C., Kalmus P., Gottlieb C. A., Thaddeus P., 1996, *ApJ*, 469, L65
- Truong-Bach Graham D., Nguyen-Q-Rieu 1993, *A&A*, 277, 133
- Tulej M., Kirkwood D. A., Pachkov M., Maier J. P., 1998, *ApJ*, 506, L69
- Ulich B. L., Haas R. W., 1976, *ApJS*, 30, 247
- Van Orden A., Saykally R. J., 1998, *Chemical Reviews*, 98, 2313
- Wakelam V., et al., 2012, *ApJS*, 199, 21
- Wakelam V., et al., 2015, *ApJS*, 217, 20
- Weltner W., Van Zee R. J., 1990, *Journal of Molecular Structure*, 222, 201
- Winnewisser G., Walmsley C. M., 1979, *Ap&SS*, 65, 83
- Zack L. N., Maier J. P., 2014, in Cami J., Cox N. L. J., eds, *IAU Symposium Vol. 297*, IAU Symposium. pp 237–246, doi:10.1017/S1743921313015949
- von Helden G., Kemper P. R., Gotts N. G., Bowers M. T., 1993, *Science*, 259, 1300

This paper has been typeset from a \LaTeX file prepared by the author.